



OPEN

GDNF/GFRA1 signaling contributes to chemo- and radioresistance in glioblastoma

Inès C. N. Avenel^{1,2,3}, Jesper D. Ewald^{4,6}, Jérémy Arieu-Bonnet^{3,7}, Ida H. Kristensen^{1,2,3}, Stine A. Petterson^{4,5}, Martin N. Thesbjerg⁵, Mark Burton⁵, Mads Thomassen⁵, Krister Wennerberg^{3,7}, Signe R. Michaelsen^{1,2,3,7,8} & Bjarne W. Kristensen^{1,2,3,7,8}✉

Glioblastoma is the most common primary brain tumor in adults, characterized by an inherent aggressivity and resistance to treatment leading to poor prognoses. While some resistance mechanisms have been elucidated, a deeper understanding of these mechanisms is needed to increase therapeutic efficacy. In this study we first discovered glial-cell derived neurotrophic factor (GDNF) to be upregulated in patient-derived glioblastoma spheroid cultures after chemotherapeutic temozolomide treatment, through RNA-Seq experiments. Therefore, we investigated the role of the GDNF/GDNF receptor alpha 1 (GFRA1) signaling pathway as a resistance mechanism to chemotherapy with temozolomide and lomustine, as well as irradiation using patient-derived glioblastoma spheroid cultures. With qPCR experiments we showed a consistent upregulation of GDNF and its primary receptor GFRA1 following all three lines of treatment. Moreover, CRISPR/Cas9 knock-outs of GDNF in two patient-derived models sensitized these cells to chemotherapy treatment, but not radiotherapy. The increased sensitivity was completely reversed by the addition of exogenous GDNF, confirming the key role of this factor in chemoresistance. Finally, a CRISPR KO of GFRA1 demonstrated a similar increased sensitivity to temozolomide and lomustine treatment, as well as radiotherapy. Together, our findings support the role of the GDNF/GFRA1 signaling pathway in glioblastoma chemo and radioresistance.

Glioblastoma is the most common primary brain tumor in adults¹. It is particularly aggressive, with a median overall survival of only 12–15 months despite treatment efforts consisting of surgical resection, followed by combined radio and chemotherapy with the alkylating agent temozolomide^{2,3}. There is no clear standard of care after glioblastoma inevitably recurs, although some patients will receive additional chemotherapy with the alkylating agent lomustine^{4,5}. Glioblastoma remains incurable, and while numerous challenges in its treatment have been reported, including MGMT-driven DNA repair and the overexpression of ATP-Binding Cassette drug efflux pumps, there is a clear need for further research into glioblastoma resistance mechanisms to improve the current treatment outcomes^{6–8}.

Glial-cell derived neurotrophic factor (GDNF) is a member of the GDNF family of ligands, with a role in supporting the survival and differentiation of dopaminergic neurons⁹. GDNF is secreted by neurons in healthy brains, and by glial cells in response to brain injuries caused by mechanical disruption or autoimmune processes¹⁰. In the classical signaling pathway GDNF homodimers bind to the GDNF receptor alpha (GFRA) isoform GFRA1¹¹, and the GDNF-GFRA1 complex binds to the rearranged during transfection (RET) receptor tyrosine kinase, activating numerous signaling pathways and triggering cell survival, proliferation, differentiation, and migration^{12–14}. Alternate RET-independent signaling routes have been described, with the GDNF-GFRA1 complex binding to neural cell adhesion molecule (NCAM) and activating the Fyn and FAK pathways, causing Schwann cell migration, adhesion, and growth¹⁵. Additionally, GDNF can signal independently of the

¹Department of Pathology, Bartholin Institute, Rigshospitalet, Copenhagen, Denmark. ²Department of Clinical Medicine, University of Copenhagen, Copenhagen, Denmark. ³Biotech Research and Innovation Centre (BRIC), University of Copenhagen, Copenhagen, Denmark. ⁴Department of Pathology, Odense University Hospital, Odense, Denmark. ⁵Clinical Genome Center, Department of Clinical Research, University of Southern Denmark Odense, Odense, Denmark. ⁶Pathology Research Unit, Department of Clinical Research, University of Southern Denmark Odense, Odense, Denmark. ⁷DCCC Brain Tumor Center, Rigshospitalet, Copenhagen University Hospital, Copenhagen, Denmark. ⁸These authors contributed equally: Signe R. Michaelsen and Bjarne W. Kristensen. ✉email: bjarne.winther.kristensen.01@regionh.dk

GFRA1 receptor by binding to Syndecan-3 and triggering the activation of the Src pathway, leading to neurite outgrowth^{16,17}.

GDNF contributes to glioma pathogenesis in various ways, making it a particularly interesting target in the investigation of glioblastoma¹⁸. Indeed, GDNF and GFRA1 are overexpressed in glioblastoma, increase angiogenesis, and contribute to the proliferation, invasion, and migration of glioma cells through the upregulation of matrix metalloproteinases^{19–21}. Finally, GDNF has been investigated as a protecting factor against carmustine, an alkylating agent previously used in glioblastoma treatment with similar effects to temozolomide and lomustine in two conventional glioblastoma cell lines, A172 and LN-229²². GDNF has been similarly associated to temozolomide resistance through siRNA experiments in the U251 human glioblastoma cell line, although the underlying mechanism remains unclear²³.

Considering this information and initial RNA-Seq experiments demonstrating an increased GDNF expression after temozolomide treatment in patient-derived glioblastoma spheroid cultures, we hypothesized that GDNF plays a role in a resistance mechanism to treatment with temozolomide, lomustine and irradiation. The objective of this study was to explore this potential resistance mechanism by quantifying the expression levels of GDNF and its receptors after treatment, as well as implementing CRISPR/Cas9 knock-outs of both GDNF and GFRA1 in two patient-derived glioblastoma spheroid cultures to investigate their response to all three lines of glioblastoma treatment.

Results

GDNF and GFRA1 are differentially expressed in patient-derived glioblastoma spheroid cultures after treatment with the alkylating agent temozolomide

This project was conducted using five patient-derived primary glioblastoma spheroid cultures; characteristics of the original patient, tumors and derived spheroid cultures are shown in Table 1. Preliminary RNA-Seq experiments were used to investigate potential genes of interest in glioblastoma treatment resistance, using 3 patient-derived spheroid cultures treated with 50 μ M temozolomide for 48 h and comparing their gene expression level to untreated counterparts. This experiment allowed us to select GDNF as a potential gene of interest, as the results showed an increased GDNF gene expression in treated T78 and T86 cells, with fold changes of 20.5 and 2.6 respectively, while GDNF expression was slightly decreased in temozolomide-treated T111 cells, with a fold-change of 0.8 (Fig. 1a). Based on these results, it was hypothesized that GDNF could contribute to a resistance mechanism to temozolomide treatment in some glioblastoma cells.

As glioblastomas are notoriously heterogeneous, we used qPCR experiments to determine the baseline expression levels of GDNF and its main receptor GFRA1 in four of the available patient-derived glioblastoma spheroid cultures. The mRNA fold changes were calculated relative to the T78 cells gene expression levels; therefore, these results do not allow for a quantitative understanding of the individual expression levels. Nonetheless, we were able to classify the spheroid cultures into two main groups: low-expressors, including T78 and T87 showing reduced expression levels of the genes of interest, and high-expressors, T105 and T111 (Fig. 1b). As GDNF is secreted from the cells, we were not able to produce IHC stainings for this protein, but spheroid clot stainings of GFRA1 show a similar pattern to the qPCR results, with a low to very low membrane GFRA1 expression in T78 and T87 respectively, and a much higher expression level in both T105 and T111 (Fig. 1c, control stainings and IHC quantifications in Fig. S2a, b, c). Analysis of survival data from TGCA showed no association between high GDNF and GFRA1 expression in IDH wildtype GBM (Figs. S2a, b), and a significant association between high GDNF expression and prolonged survival in the inherently resistant to TMZ MGMT unmethylated subgroup of IDH WT GBM (Fig. S1c).

GDNF expression increases in response to three glioblastoma lines of treatment: temozolomide, lomustine and irradiation

To confirm the increased GDNF expression seen in the RNA-seq experiment, T78, T87 and T105 cells were exposed to 50 μ M of temozolomide and T111 to 100 μ M of temozolomide, to quantify mRNA fold changes relative to a DMSO control. As preliminary experiments proved T111 cells to be more resistant to TMZ compared to the other cell lines used in this experiment, a higher dose of TMZ was needed to induce comparable responses across cell lines. After 48 h of treatment, there was a significant increase in GDNF expression in T78, T87 and T105 cells (p -value ≤ 0.0001 ; Fig. 2a–c), and while T111 GDNF expression was slightly elevated, it was not significant (Fig. 2d). The fold changes varied across spheroid cultures, ranging from 1.2 for T111 to 23.2 for T105. This increased gene expression pattern in response to temozolomide treatment was similarly seen for the GFRA1 receptors in all four spheroid cultures, although it was only statistically significant in T87 (p -value ≤ 0.05 ; Fig. 2b).

Spheroid culture	Age at diagnosis	Sex	Subtype	MGMT methylation status	p53	EGFR	NGS mutations
T78	56	M	Mesenchymal	Methylated	N/A	N/A	N/A
T86	81	M	Classical	Unmethylated	low	+	N/A
T87	82	M	Proneural	Methylated	+	+	N/A
T105	70	F	N/A	Methylated	+	+	PTEN (V85D)
T111	61	F	Mesenchymal	Methylated	+	+	N/A

Table 1. Characteristics of patient-derived primary glioblastoma spheroid cultures.

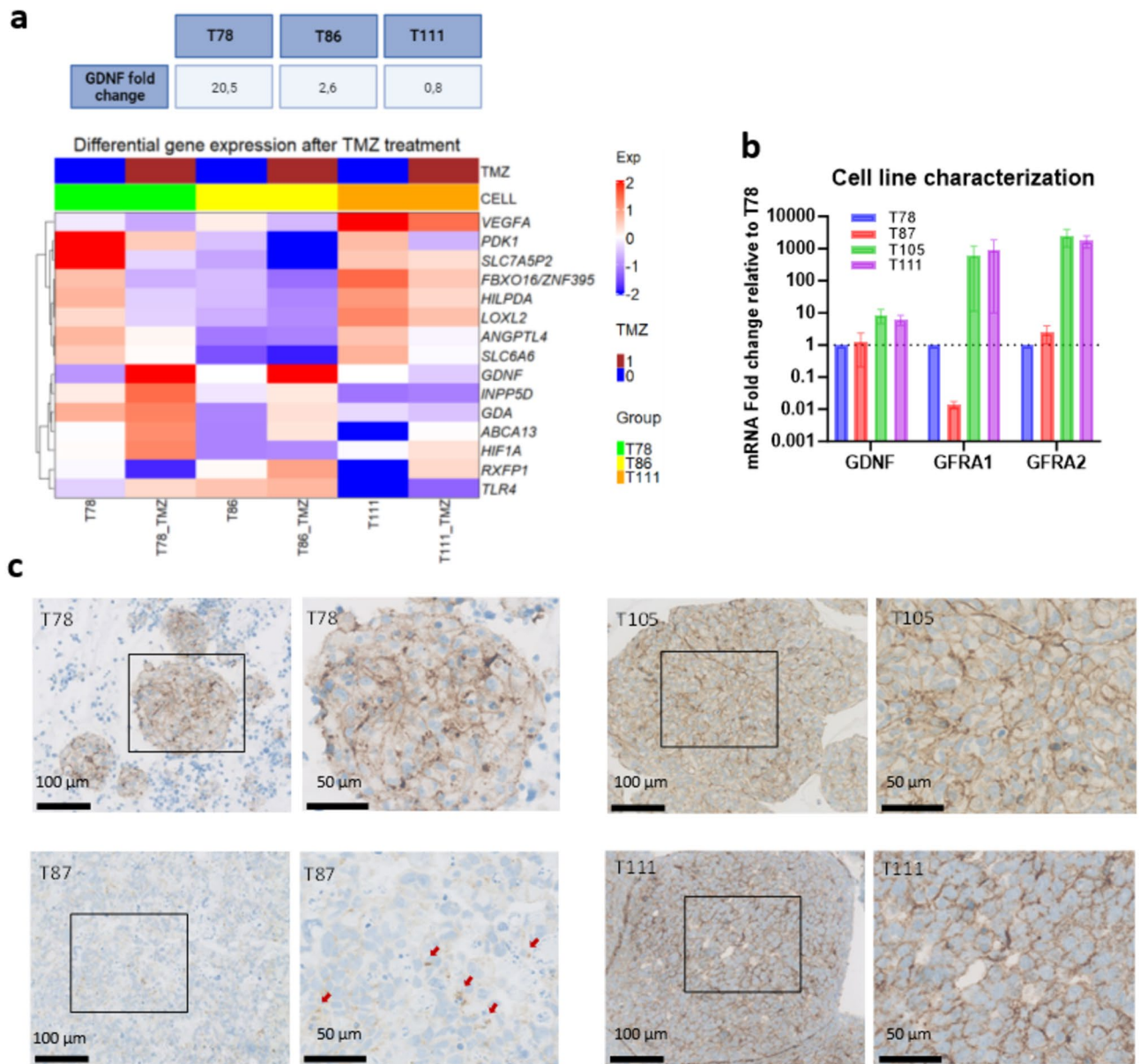


Figure 1. Expression of GDNF and GFRA1 in four glioblastoma patient-derived spheroid cultures. (a) Heatmap representation of the top 15 differentially expressed genes in response to treatment with 50 μM of temozolomide in three patient-derived glioblastoma spheroid cultures, T78, T86 and T111. Associated table showing the fold change in GDNF expression for all three cell types. (b) Relative baseline expression of GDNF and its associated receptor GFRA1 in four patient-derived glioblastoma spheroid cultures: T78, T87, T105 and T111. RNA gene expression of cells cultured in serum-free NB media, as measured with qPCR. mRNA fold change calculated to be relative to T78 expression levels, standardized to 1 ($n=3$, mean \pm SEM). (c) Immunohistochemical stainings of 3D spheroid sections reveal varying expression of GFRA1 across four patient-derived glioblastoma spheroid cultures. Nuclei counter stained with hematoxylin. Red arrows showing some membrane staining in the T87 augmented picture. Scale bars: 100 μm for the original image (left) and 50 μm in the augmented image (right).

Due to the greater availability of some cells, we proceeded with only two spheroid cultures of each category for the remainder of the study: the low-expressor T87, and the high-expressor T111.

To determine if similar results could be obtained after treatment with another alkylating agent used in glioblastoma treatment, the two spheroid cultures were treated with 40 and 60 μM of lomustine and harvested after 48 h of treatment. As shown in Fig. 2e, in the T87 cells, the treated samples showed an almost two-fold significant increase in GDNF expression ($p\text{-value} \leq 0.05$) after treatment with both concentrations of lomustine. In T111 cells, only treatment with 60 μM of lomustine resulted in a statistically significant increase in GDNF production ($p\text{-value} \leq 0.05$), although a slight non-significant increase was also observed after treatment with the lower dose of lomustine (Fig. 2f). This minor increase in gene expression also applied to GFRA1, although variations

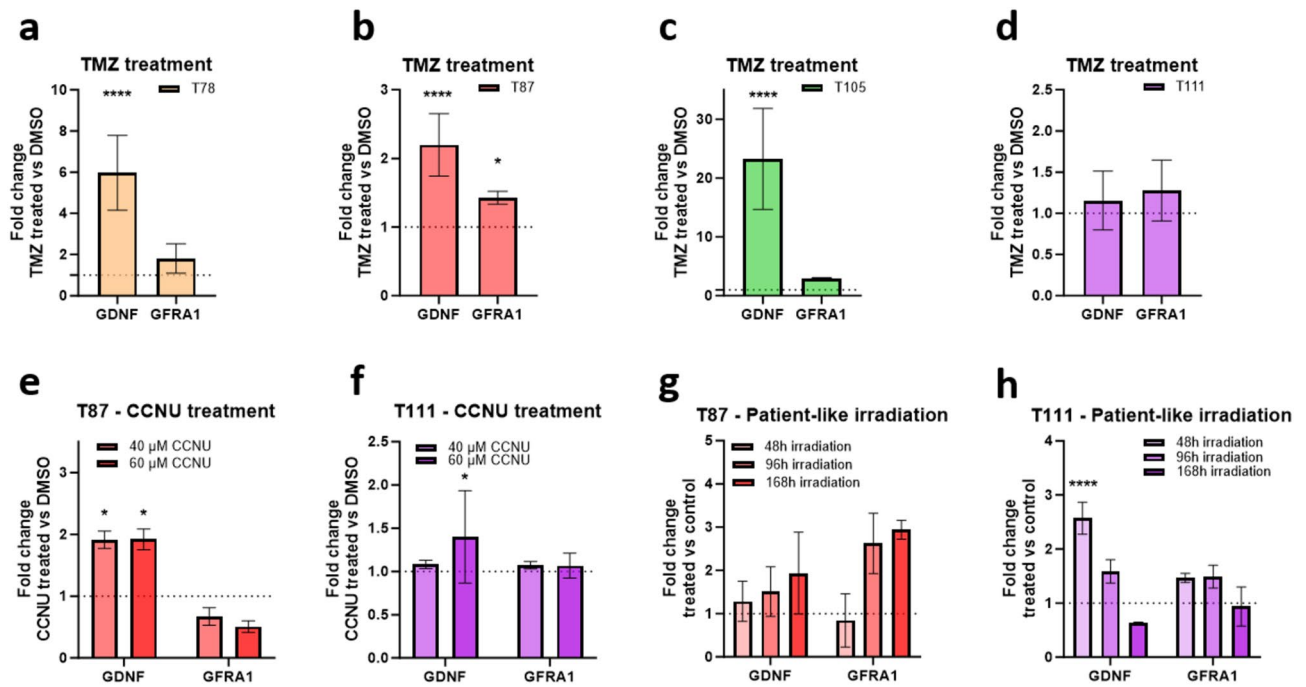


Figure 2. Increased GDNF/GFRA expression in response to three lines of glioblastoma treatment. (a–d) Relative expression of GDNF and GFRA1 in four patient-derived glioblastoma spheroid cultures after treatment with 50 μM of temozolomide (TMZ) for T78, T87 and T105 and 100 μM TMZ for T111. (e, f) Relative expression of GDNF and GFRA1 in T87 and T111, after treatment with 40 or 60 μM of lomustine (CCNU). RNA gene expression as measured with qPCR, mRNA fold change calculated to be relative to expression levels of a DMSO control, standardized to 1 and represented by a dotted line ($n = 3$, mean \pm SEM). (g, h) Relative expression of GDNF and GFRA1 in two patient-derived glioblastoma spheroid cultures, T87 and T111, after treatment with a patient-like irradiation schedule of 2 Gy per day for 5 consecutive days. Samples were harvested at 3 timepoints following the last round of irradiation: 48h, 96h and 168h. In all experiments, RNA gene expression was measured with qPCR, mRNA fold changes were calculated to be relative to the expression levels of a DMSO or non-irradiated control harvested at the same timepoints, all standardized to 1 and represented by a dotted line ($n = 3$, mean \pm SEM). * = $p \leq 0.05$, ** = $p \leq 0.01$, *** = $p \leq 0.001$, **** = $p \leq 0.0001$ with two-way ANOVA analysis.

in the mRNA production of this gene may be more difficult to assess due to its higher baseline expression levels (Fig. 1c).

Finally, to investigate the cellular responses to irradiation, both spheroid cultures were subjected to a patient-like irradiation schedule of 2 Gy per day for five consecutive days. Samples were harvested 48, 96 and 168 h after the last round of irradiation and the mRNA fold changes were calculated relative to non-irradiated control harvested at the same respective timepoints. Both spheroid cultures exposed to continued irradiation showed a pattern of heightened GDNF and GFRA1 expression. While this increase was not significant in T87 cells (Fig. 2g), T111 cells showed a statistically relevant 2.5-fold increase in GDNF expression after 48 h (p -value ≤ 0.0001) and GDNF was upregulated although not significantly at the 96-h timepoint (Fig. 2h). This increased but non-significant expression pattern after irradiation was found for both genes in T111 cells, with the exception of the 168-h timepoints (Fig. 2h).

CRISPR KO of GDNF does not affect cell viability alone but sensitizes cells to alkylating agent chemotherapy

To investigate the role of GDNF in resistance to treatment, we transfected both T87 and T111 Cas9 expressing cells with either a non-targeting control sgRNA (NTC1), or three separate GDNF KO sgRNAs. To confirm the efficacy of the transfection and as GDNF is a secreted compound, we performed an ELISA assay using conditioned media from GDNF-producing control cells (NTC1), and all three KO spheroid cultures, for both T87 and T111. For T87, the ELISA assays showed the following statistically significant reductions in GDNF production, relative to the NTC1 control: 56% for KO1 (p -value ≤ 0.001), 33% for KO2 (p -value ≤ 0.05) and 65% for KO3 (p -value ≤ 0.001) (Fig. 3a). The same pattern was found in T111 cells, with the following statistically significant reductions in GDNF production: 77% for KO1 (p -value ≤ 0.001), 48% for KO2 (p -value ≤ 0.01) and 78% for KO3 (p -value ≤ 0.001) (Fig. 3b). MTT assays were conducted after the transfection process to determine if the loss of GDNF expression had any effect on cell viability. For both the T87 and T111 spheroid cultures, none of the GDNF KO sgRNAs showed a statistically relevant difference in cell viability, when compared to the GDNF-producing NTC1 cells (Fig. 3c, d).

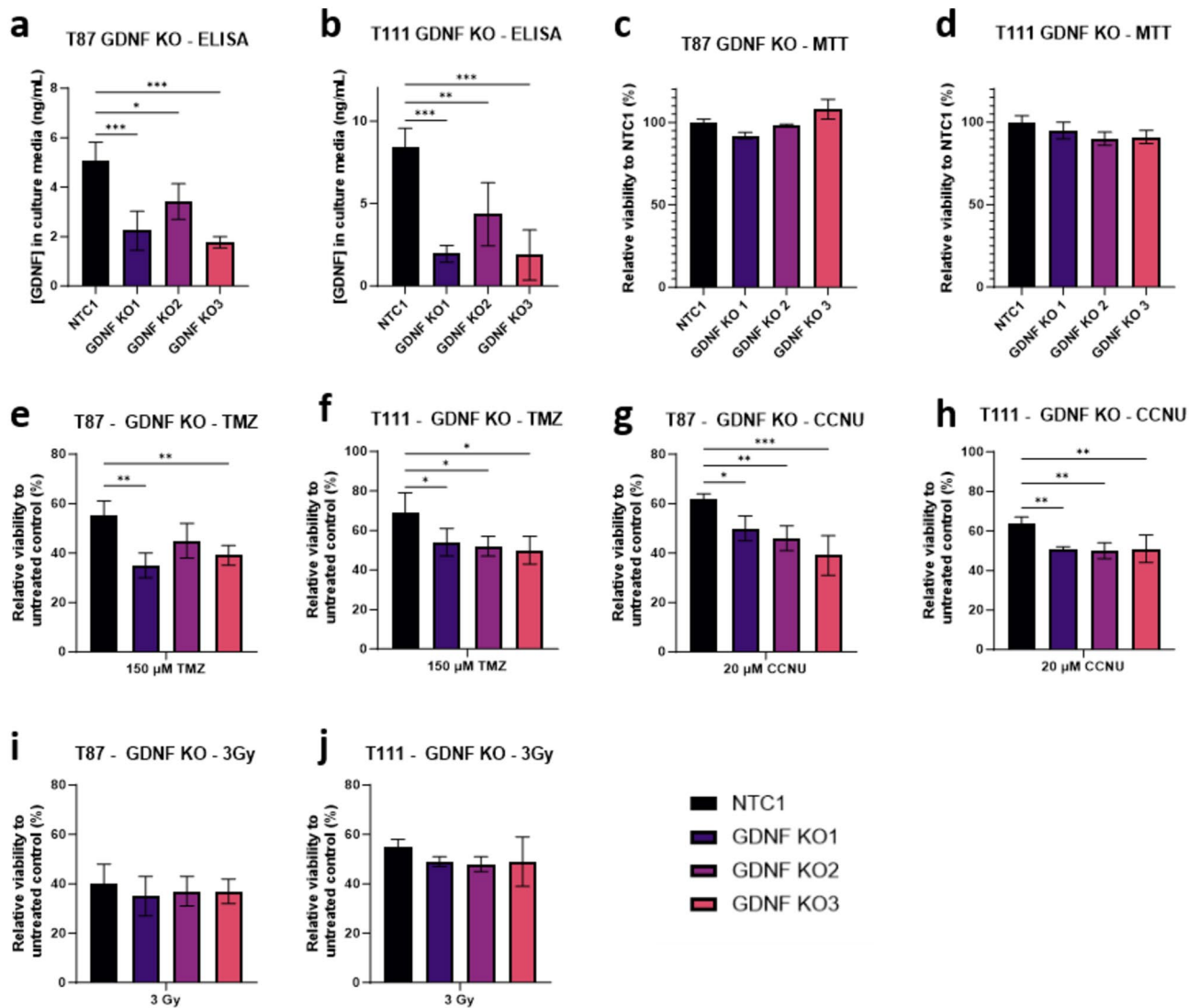


Figure 3. CRISPR KO of GDNF does not affect cell viability alone but leads to increased cell sensitivity after treatment with temozolomide (TMZ) and lomustine (CCNU). (**a, b**) ELISA assays showing significantly decreased GDNF concentrations in conditioned culture media from GDNF KO cells lines, compared to the NTC1 control in two cell types, T87 (left) and T111 (right), ($n=3$, mean \pm SEM). (**c, d**) CRISPR KO of GDNF does not significantly reduce cell viability in T87 (left) and T111 (right). MTT assays representing cell viability of each GDNF-KO cell type respective to the GDNF producing NTC1 controls. ($n=10$, mean \pm SD). (**e, f**) MTT assays showing mostly significantly decreased cell viability of T87 and T111 GDNF KO cells compared to their respective NTC1 controls, after treatment with 150 μ M of TMZ. The comparison of viability between T87 NTC1 and GDNF KO2 was borderline significant, with a p -value of 0.06. ($n=3$, mean \pm SEM) (**g, h**) MTT assays showing significantly decreased cell viability of T87 and T111 GDNF KO cells compared to their respective NTC1 controls, after treatment with 20 μ M of CCNU. ($n=3$, mean \pm SEM). (**i, j**) MTT assays showing a slight but non-significant decrease in cell viability of T87 and T111 GDNF KO cells compared to their respective NTC1 controls, after treatment with 3 Gy of irradiation. ($n=3$, mean \pm SEM). Statistical analysis with one-way ANOVA: * = $p \leq 0.05$, ** = $p \leq 0.01$, *** = $p \leq 0.001$, **** = $p \leq 0.0001$.

Finally, to investigate the effect of GDNF loss in treatment resistance we compared post-treatment viability of the GDNF-KO spheroid cultures to NTC1 after treatment either 150 μ M of temozolomide, 20 μ M of lomustine, or 3 Gy of radiation. After temozolomide treatment, most KO cell models for both T87 and T111 showed a statistically significant decrease in post-treatment viability, ranging from 20% for T87 KO1 (p -value ≤ 0.01 , Fig. 3e) to 15% for T111 KO1 (p -value ≤ 0.05 , Fig. 3f). Only the T87 KO2 10% decrease in post-treatment viability was borderline significant when compared to the NTC1 control, with a p -value of 0.06. After lomustine treatment, all KO cells models showed a statistically significant decrease in post-treatment viability, ranging from 23% for T87 KO3 (p -value ≤ 0.001 , Fig. 3g) to 12% for T87 KO1 (p -value ≤ 0.05 , Fig. 3h). Although a small decrease in viability ranging from 3 to 7% was observed in the KO cells models after irradiation with a dose of 3 Gy, none of these differences were statistically significant when compared to the GDNF-expressing control NTC1 (Fig. 3i, j).

Addition of exogenous GDNF reverses the increased post-treatment sensitivity in the GDNF-KO spheroid cultures

To confirm that the increased post-treatment sensitivity observed in Fig. 3e–h was indeed due to the loss of GDNF, we modified this experiment to add another condition: treatment with both temozolomide or lomustine and 1 µg/ml of exogenous GDNF. Since the results of the irradiation experiments did not indicate a clear effect of GDNF in radiation treatment resistance, this treatment modality was not included in this experiment.

After temozolomide treatment (Fig. 4a, b), all T87 and T111 GDNF-KO cells lines showed a clear decrease in post-treatment viability compared to their respective NTC1 controls, ranging from 4% for T87 KO3 to 22% for T111 KO1. After combined treatment with both temozolomide and GDNF, the viability of the NTC1 controls was similar to their equivalents treated uniquely with temozolomide, whereas there was a statistically significant increase in viability when comparing the GDNF KO spheroid cultures to these same GDNF KO cells after supplementation with exogenous GDNF. The viability increases due to the GDNF addition ranged from 7% for T87 KO3 (p -value ≤ 0.05) to 15% for T111 KO1 (p -value ≤ 0.0001), and reached viability values equal to or slightly higher than the NTC1 control. The same pattern was found in both T87 and T111 after lomustine treatment (Fig. 4c, d), with post-treatment viability decreases reaching 20% for T111 KO2, and post GDNF-treatment viability increases ranging from 8% for T111 KO3 (p -value ≤ 0.05) to 21% for T87 KO1 (p -value ≤ 0.0001).

CRISPR KO of GFRA1 impacts both pre and post treatment cell viability

To determine if the GDNF-related protective effect was associated with its main GFRA1-dependent signaling route, we performed a CRISPR/Cas9 KO of the GFRA1 receptor in T87 and T111 cells. As for the GDNF KO, the viability of GFRA1 NTC1 control and KO cells was assessed with an MTT assay. In this case, all KO spheroid

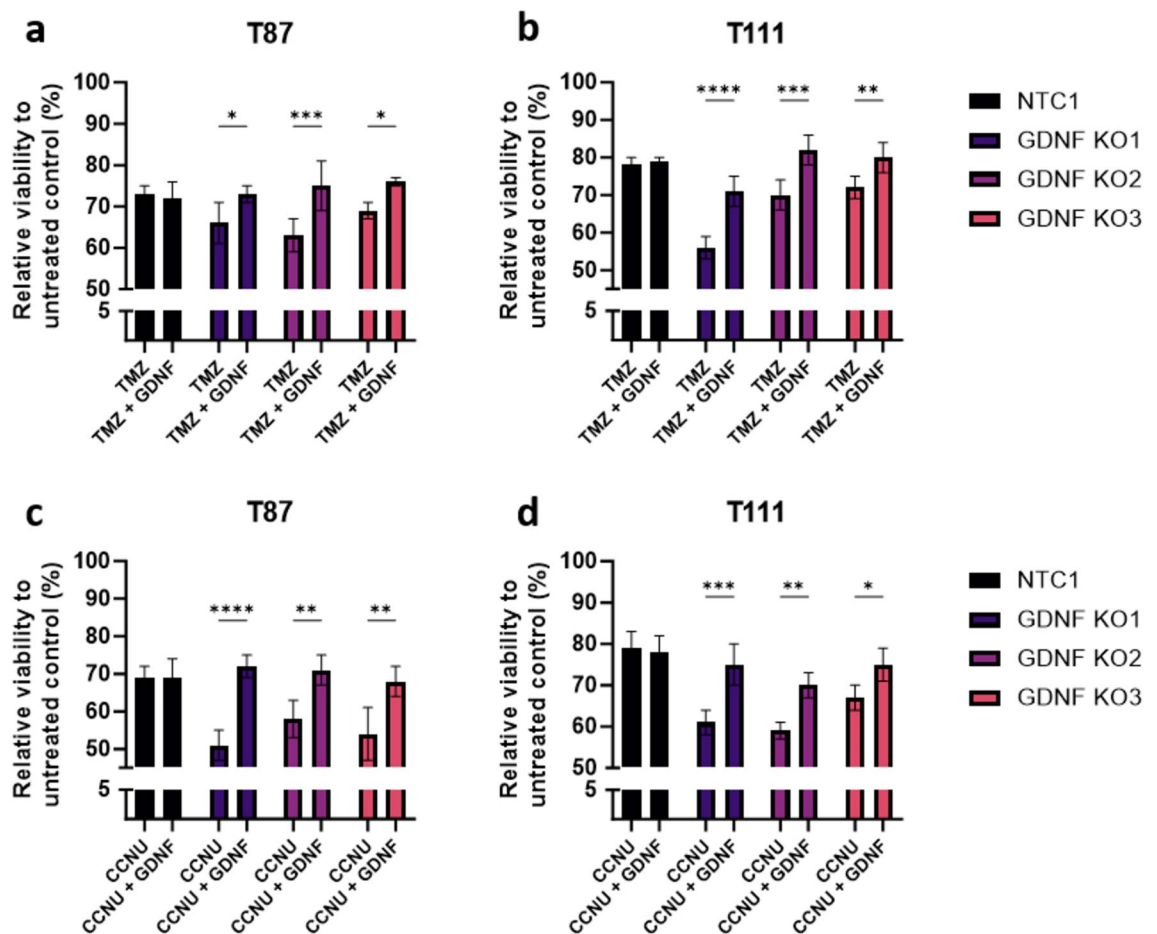


Figure 4. Increased sensitivity to temozolomide (TMZ) and lomustine (CCNU) treatment in GDNF KO spheroid cultures can be reversed by the addition of exogenous GDNF. (a, b) MTT Rescue experiments showing significantly increased post-treatment viability after addition of 1 µg/ml exogenous GDNF in T87 and T111 GDNF KO cells, but not in NTC1 controls, after treatment with 150 µM TMZ. DMSO and MilliQ water were used as controls for TMZ and GDNF respectively ($n = 3$, mean \pm SEM). (c, d) MTT Rescue experiments showing significantly increased post-treatment viability after addition of 1 µg/ml exogenous GDNF in T87 and T111 GDNF KO cells, but not in NTC1 controls, after treatment with 20 µM CCNU. DMSO and MilliQ water were used as controls for CCNU and GDNF respectively. ($n = 3$, mean \pm SEM). Statistical analysis with one-way ANOVA: * = $p \leq 0.05$, ** = $p \leq 0.01$, *** = $p \leq 0.001$, **** = $p \leq 0.0001$.

cultures except T111 KO1 showed a significant decrease in viability compared to their GFRA1 producing counterparts (Fig. 5a, b). As the cell viability was similar across the cell types during their overtime culture, we hypothesize that this viability difference is due to a slower growth rate of the KO spheroid cultures. This supposed slower cell growth does not have an effect on any of the subsequent experiments as protein concentration was normalized across all samples in the Western Blot validation of the KO, and the viability of each spheroid culture was calculated relative to the untreated control of the same cell type in the post-treatment viability experiments.

The knock-out was validated with the Jess digital capillary-based Western Blotting system (Biotechne) for both T87 and T111 and showed a consistently decreased GFRA1 expression in all KO spheroid cultures, although with varying efficacies (Fig. 5c, d; Full capillary readouts in Figs. S3a, b). As GFRA1 is a membrane receptor, the KO could also be validated with IHC stainings of spheroid clots. As the baseline GFRA1 IHC stainings of T87 were very faint (Fig. 1c), the T87 GFRA1-KO spheroid cultures were not included in this experiment. For T111, the NTC1 control spheroid clot showed a defined delineation of each cell with specific membrane staining of the receptor, while the KO spheroid cultures showed some unspecific background staining of the clot, and varying amounts of membrane staining around individual cells, although decreased compared to the control, corresponding to cells that have not successfully undergone the transfection process (Fig. 5e). After quantification of these IHC stainings, the average GFRA1 stain area was significantly reduced (p -values ≤ 0.0001 , Fig. S2d) in all T111 GFRA1 KO spheroid cell clots, compared to the T111 NTC1 cell clots.

Finally, to investigate the role of GDNF/GFRA1 signaling in the potential resistance mechanism to treatment, both GFRA1-expressing NTC1 controls and GFRA1-KO T87 and T111 spheroid cultures were exposed to treatment with either 150 μ M of temozolomide, 20 μ M of lomustine, or 3 Gy of radiation. Although no clear protective effect of GDNF against irradiation was previously found (Figs. 3i, j), we repeated these experiments with the GFRA1 KO. After temozolomide treatment, most KO cells models showed a statistically significant decrease in post-treatment viability, ranging from 6% for T87 KO1 and KO2 (p -values ≤ 0.05 , Fig. 5f) to 13% for T111 KO3 (p -value ≤ 0.01 , Fig. 5g). Similarly, after lomustine treatment, most KO cells models showed a statistically significant decrease in post-treatment viability, from 10% for T87 KO1 (p -value ≤ 0.05 , Fig. 5h) to 16% for T111 KO3 (p -value ≤ 0.01 , Fig. 5i). Finally, while GDNF loss had no significant effect on post-irradiation viability, all GFRA1 KO cells models except T111 KO1 showed a statistically significant decrease in post-treatment viability, from 5% for T87 KO3 (p -value ≤ 0.05 , Fig. 5j) to 12% for T111 KO2 and KO3 (p -values ≤ 0.01 , Fig. 5k).

Discussion

In this study, we investigated the role of GDNF/GFRA1 signaling in glioblastoma resistance to treatment using CRISPR/Cas9 technology and patient-derived glioblastoma spheroid cultures. We first discovered GDNF as a gene of interest following RNA-Seq experiments showing increased GDNF expression after temozolomide treatment in two patient-derived glioblastoma spheroid cultures. While numerous promising glioblastoma targets have been discovered owing to gene editing, to our knowledge only a few studies have investigated the role of GDNF in this disease, and the available GDNF gene editing studies in glioblastoma used transient siRNA techniques instead of the irreversible CRISPR/Cas9 system^{19,21,23,24}. Moreover, most available GDNF glioblastoma studies were performed using conventional cell lines grown in serum-supplemented media^{21,22,24–26}. Culturing of glioblastoma cells in serum-containing media has been shown to induce a dramatic and non-reversible cell morphology change, the formation of a highly homogeneous monolayer of cells, and the loss of their self-renewal and differentiation abilities²⁷. In contrast, spheroid-cultures have the advantage of providing a similar cell environment to the in vivo tumor, maintaining intrinsic tumor cell phenotypes, improving cell viability and proliferation, and promoting stemness marker expression through the secretion of neurotrophic factors, cytokines, and chemokines²⁸. Therefore, in this study we chose to use patient-derived spheroid cultures with a reduced passage number and cultured without serum, to approximate the original tumor characteristics as closely as possible. Furthermore, given the high heterogeneity of glioblastoma²⁹, we selected two patient-derived spheroid cultures with very different baseline expression levels of GDNF and its receptor to investigate if this prospective resistance phenomenon is an overall characteristic of glioblastoma, or patient tumor-specific.

While investigating the effect of temozolomide, lomustine and irradiation treatment on glioblastoma tumor cells, we found different response patterns across spheroid cultures, with the high-expressor T111 having consistently lower expression levels of the genes of interest after treatment, compared to the low-expressor T87. This could be a reflection of the higher baseline levels of these genes in this cell type, complicating the assessment of smaller variations in gene expression. Interestingly, CRISPR/Cas9 whole-genome screens of patient-derived glioma stem cells (GSC) with or without temozolomide treatment established that while GSC-specific pathways with roles in DNA repair, cell cycle and chromatin organization were conserved in most tumors, a number of temozolomide resistance targets were not conserved across patient-samples suggesting the existence of preferential temozolomide resistance pathways in different patients³⁰. In our experiments, after lomustine treatment the same overall fold change difference was present, but in addition T87 cells showed a clear decrease in GFRA1 expression which was not present in T111 cells. This could be due to a negative feedback mechanism decreasing GFRA1 receptor expression in response to increased ligand expression. Finally, after the patient-like irradiation assay, the expression levels of both GDNF and its receptors increased in T87 cells in a time-dependent manner, while they decreased in T111 cells. From these results, we hypothesize that the existence of patient-specific preferential resistance pathways may extend to the other available forms of glioblastoma treatment, including irradiation. Additionally, this difference in baseline gene expression and post-treatment behavior might be linked to either the gender of the patient or the subtype of the tumor, as both cell lines have the same MGMT methylation status, p53 and EGFR amplifications and do not harbor any cell line specific genetic mutations. Indeed, T87 cells were derived from a male patient and T111 cells from a female patient, and T87 is a proneural glioblastoma while T111 is mesenchymal. Interestingly, these subtypes have been associated with differing survival times,

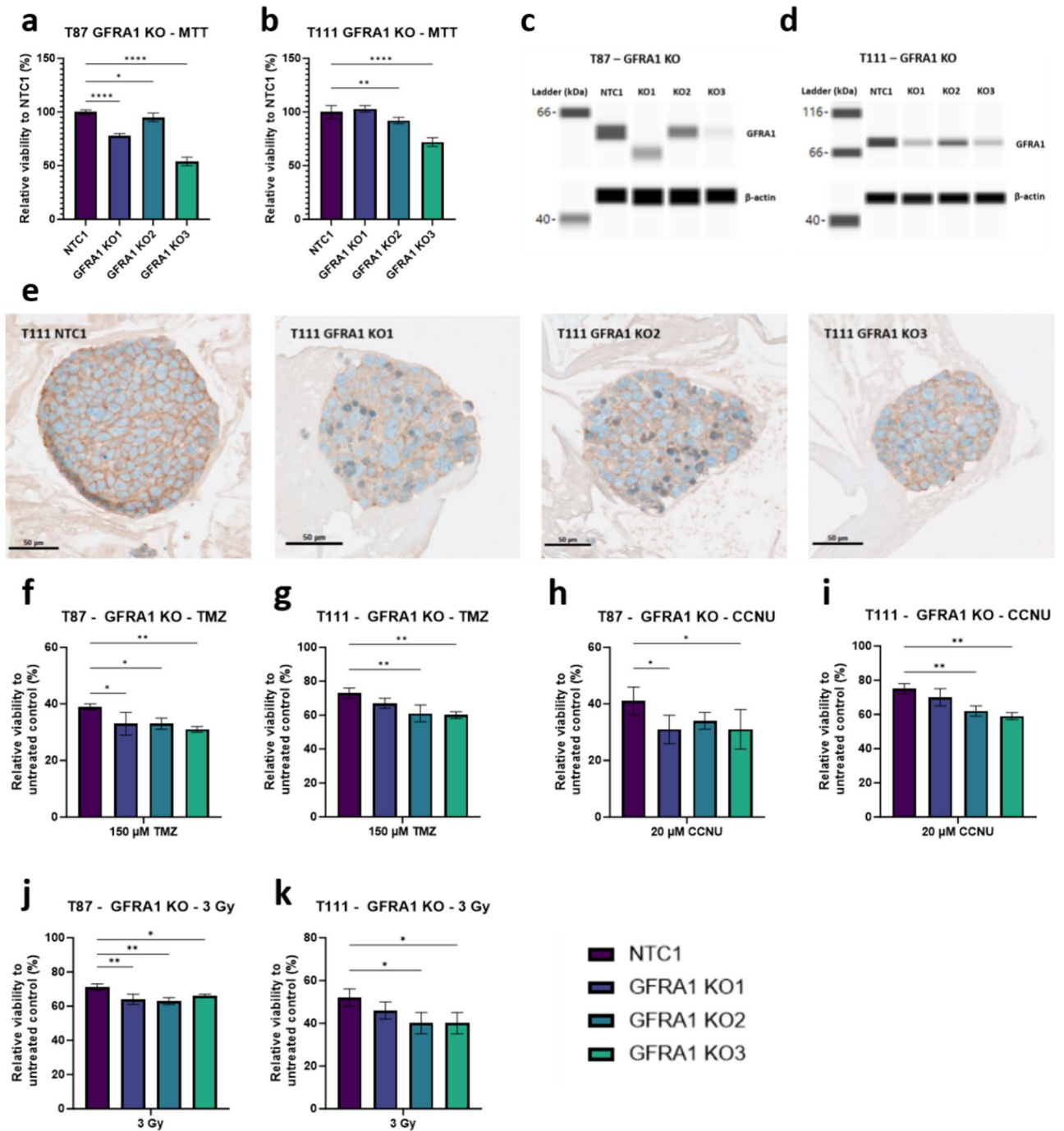


Figure 5. CRISPR KO of GFRA1 decreased baseline cell viability and leads to increased cell sensitivity after treatment with temozolomide, lomustine and irradiation (**a, b**) CRISPR KO of GFRA1 significantly reduced cell viability in most T87 (left) and T111 (right) knock-outs. MTT assays representing cell viability of each GFRA1-KO spheroid culture respective to the GFRA1 expressing NTC1 controls. ($n = 10$, mean \pm SD). (**c, d**) Capillary-based Western Blot demonstrating reduced GFRA1 protein expression levels in the T87 (left) and T111 (right) GFRA1-KO cells, compared to the NTC1 controls. β -actin used as a loading control. (**e**) IHC stainings of 3D spheroid sections reveal lower expression of GFRA1 in the T111 KO cells, compared to the GFRA1 expressing NTC1 cells. Nuclei counter stained with hematoxylin. Scale bars: 50 μ m (**f, g**) MTT assays showing mostly significantly decreased cell viability of T87 and T111 GFRA1 KO spheroid cultures compared to their respective NTC1 controls, after treatment with 150 μ M of TMZ. ($n = 3$, mean \pm SEM) (**h, i**) MTT assays showing significantly decreased cell viability of two T87 and T111 GFRA1 KO spheroid cultures compared to their respective NTC1 controls, after treatment with 20 μ M of CCNU. ($n = 3$, mean \pm SEM). (**j, k**) MTT assays showing the same decrease in cell viability of all T87 and two T111 GFRA1 KO spheroid cultures compared to their respective NTC1 controls, after treatment with 3 Gy of irradiation. ($n = 3$, mean \pm SEM). Statistical analysis with one-way ANOVA: * = $p \leq 0.05$, ** = $p \leq 0.01$, *** = $p \leq 0.001$, **** = $p \leq 0.0001$.

with mesenchymal having the worst prognosis and proneural the best³¹. The MGMT promoter methylation status and the amplification of p53 and EGFR are common alterations in GBM, unrelated to the GDNF/GFRA1 signaling pathways¹. Therefore, these molecular features should not have an impact on GDNF-related mechanisms, and similarly the KO of both GDNF and GFRA1 should not reflect on any of the aforementioned tumor characteristics.

The results of MTT assays following the GDNF KO CRISPR transfection established that the loss of GDNF did not have an effect on glioblastoma cell viability. This finding was unexpected as the role of GDNF in promoting cell survival is widely documented³². Nonetheless, the GDNF-KO cells seemed to have a slower culture growth rate compared to the GDNF-producing control cells, which was similarly observed for the GFRA1-KO cells, as evidenced by the lower MTT viability of the KO cells compared to their control counterpart. These observations are in line with another study confirming the role of GDNF in the proliferation of rat C6 glioma cells³³.

The GDNF and GFRA1 knock-outs were validated with ELISA, Western Blot and IHC assays. In the T87 GFRA1-KO Western Blot experiments, bands at different molecular weights were observed, such as a 70 kDa band which may correspond to the N-glycosylated form of the protein³⁴, and a 57 kDa band indicative of a truncated protein, as this particular sgRNA cleaved GFRA1 at the border between the signal peptide and the mature protein. Overall, varying GDNF and GFRA1 expression levels were seen in all KO spheroid cultures, likely due to the presence of non-transfected cells or inefficient Cas9 expression in the original cell cultures. In addition, CRISPR/Cas9 edited genes may still undergo transcription and translation, resulting in the production of non-functional truncated proteins detectable with ELISA, western Blot and IHC assays³⁵. Consequently, the KO validation experiments may not precisely reflect the concentration of functional GDNF and GFRA1 in these cultures but showed a sufficient difference from the control to proceed with viability testing experiments.

In treatment experiments with GDNF KO cells, we demonstrated an increased sensitivity of these cells to chemotherapy but not to irradiation. The experimental design was based on dose testing experiments for temozolomide and lomustine and measured cell viability five days after treatment. However, this may not be ideal for irradiation experiments as double strand break repairs usually occur within 24 h after irradiation³⁶. As a viability difference might not be evidenced with MTT assays for this short of a timeline due to the inherent limitation of the cell growth rate, this experiment may benefit from an overtime monitoring of cell viability after irradiation treatment to determine if GDNF loss does indeed have an effect on radiosensitivity.

Finally, although the GFRA1-KO treatment experiments showed an increased sensitivity of the KO cells models, the post treatment viability decrease was higher in the corresponding GDNF-KO treatment experiments. This could be explained by the presence of GDNF in the culture media as well as non-successfully transfected cells expressing GFRA1 in the GFRA1-KO spheroid cultures, leading to sufficient GDNF/GFRA1 signaling to trigger the resistance mechanism. The concentration of GDNF in the brain is unclear, it has been reported as 43–70 pg/mg of protein in the brain, 218 pg/mL in cerebrospinal fluid, and 400–500 pg/mL in serum, although this last figure was measured in Parkinson's patients and therefore may not reflect the physiological concentration^{37–39}. Moreover, the physiological concentrations of GDNF in the brain may not reflect the GDNF concentration in the glioblastoma tumor microenvironment, as GDNF expression is reported to be up to 5 times higher in glioblastoma samples when compared to normal brain samples from the same patients¹⁹. A large range of experimental conditions have been used to study the effects of GDNF on glioblastoma cells, reaching up to 4 µg/mL of GDNF²⁰, and our rescue experiment showed positive results with 1 µg/mL of exogenous GDNF. Therefore, while the GFRA1 KO cells may not fully reflect the consequences of GFRA1 loss, the results of the GFRA1 treatment response experiments demonstrate that the resistance mechanism linked to GDNF is indeed due to signaling through its preferential receptor GFRA1. Preliminary experiments not pictured in this study did not show RET expression at the protein level in the patient-derived glioblastoma cell models, and therefore RET inhibition was not further investigated in this study.

All together, these results highlight the key role of the GDNF/GFRA1 signaling pathway in glioblastoma resistance to treatment, as demonstrated by CRISPR/Cas9 experiments in two distinctive patient-derived glioblastoma spheroid cultures. We obtained similar results in two patient-derived spheroid cell cultures, representing different glioblastoma subtypes and different baseline expression levels of GDNF and GFRA1, indicating that this chemo and radioresistance phenomenon is conserved across tumor types. Though we evidenced the role of GDNF/GFRA1 signaling in this process, further studies should be conducted to underscore the key signaling molecules implicated in downstream signaling, investigate the potential role of DNA damage signaling and repair in this resistance mechanism, identify novel specific GDNF/GFRA1 inhibitors through pharmacological screens and obtain in vivo information to determine how this phenomenon may be exploited to improve the currently available treatment options.

Materials and methods

Patient-derived material

The patient-derived glioblastoma cells used in this study were isolated from fresh tumor tissue after initial surgery of World Health Organization grade IV glioblastomas from May 2007 through January 2010 at the Department of Neurosurgery, Odense University Hospital, Odense, Denmark, after informed consent was obtained from the patients. The Regional Scientific Ethical Committee approved the use of human glioma tissue and cells in the present study (approval number S-20150148) and all experiments were performed in accordance with the relevant guidelines and regulations.

Cell culture

Five patient-derived primary glioblastoma spheroid cultures, T78, T86, T87, T105 and T111 were previously established⁴⁰, characterized and validated in our laboratory and were cultured in serum-free neurobasal medium

(NB) (Gibco), supplemented with 1% each Penicillin + Streptomycin (Gibco), L-Glutamine (Gibco) and B27 (Invitrogen), 0.5% N2 (Invitrogen) and 25 ng/mL each of EGF (Sigma-Aldrich) and bFGF (PeproTech). All cells were maintained at 37 °C in a humidified atmosphere of 5% CO₂.

RNA-Seq and Heatmap

4 million T78, T86 and T111 cells were treated with 50 μM of temozolomide (Sigma-Aldrich) or a DMSO (Sigma-Aldrich) control for 48 h, after which the media was removed, and the cells were grown in NB + all media for a week. Treated and untreated cells in suspension were harvested, and RNA extraction was performed using the RNeasy Mini Kit (Qiagen). RNA was converted to ds cDNA using the TrueSeq Stranded Total RNA Gold Kit (Illumina), and the ds cDNA pools were sequenced using the HiSeq 1500 System (Illumina). Bowtie2 version 2.1.0 and Tophat2 version 2.0.10 with default parameters were used to align the RNA-seq reads against the human transcriptome and genome. The output files were indexed using Samtools version 0.1.19, and Cufflinks version 2.1.1 was used for sample transcriptome assembly, transcript isoform identification and abundance estimation. Differential gene expression analysis on known UCSC genes was done using the edgeR R-package (version 3.4.2), from the R version 3.0.2 open source-environment.

qPCR

For all qPCR assays, total cell RNA was extracted with the RNeasy Plus Mini Kit and QIAshredders (Qiagen). The reverse transcription of RNA into cDNA was done using the SuperScript III First-Strand Synthesis Super-Mix (ThermoFisher Scientific). qPCR was performed using TaqMan Gene Expression Primers for GDNF and GFRA1 (ThermoFisher Scientific), with GAPDH and RPL13A as housekeeping genes, and the following cycling conditions: 50 °C for 2 min, 95 °C for 1 min, 50 cycles of 95 °C during 1 s, and finished by 20 s at 60 °C. mRNA abundance was normalized to the standard condition sample using the 2^{-ΔΔCT} method for efficiency correction. mRNA abundance was represented in Graph Pad Prism 10 (GraphPad software, San Diego, CA) as the mean fold change compared to the control conditions ± SEM for *n* = 3.

GFRA1 IHC stainings

Tumor spheroids were harvested, captured in plasma-thrombin clots, fixed in 4% paraformaldehyde, embedded in paraffin, and cut into 3 μm sections on a microtome. Sections underwent deparaffinization, followed by the blocking of peroxidase activity. Heat-induced epitope retrieval was completed, and the sections were stained with both Hematoxylin (Roche Diagnostics) and GFRA1 (sc-271546 E-11, 1:800, Santa Cruz Biotechnology). Stained slides were digitalized with the Vectra Polaris Automated Quantitative Pathology Imaging System (Akoya Biosciences).

Software-based cell classification and quantification

The digitalized slides were imported into the Visiopharm software V2018.9.4 and a classifier detecting different staining intensities of GFRA1 were created via a threshold-based approach. The total stained area fraction was measured by the formula: (fraction of stained area)/(total area).

Cell treatment assays

Temozolomide and lomustine treatment assays

1 million T78, T87, T105 and T111 single cells were grown to 100 to 200 μm spheroids. T78, T87 and T105 spheroids were treated with either 50 μM temozolomide or an equivalent DMSO solution, and T111 cells were treated with 100 μM temozolomide or DMSO. After 48 h, cells were harvested for RNA purification and qPCR. A similar protocol was implemented for the lomustine (Sigma-Aldrich) treatment assays, with T87 and T111 100–200 μm spheroids being treated with both 40 and 60 μM of lomustine, or an equivalent DMSO solution. Similarly, 48 h after treatment, cells were harvested for RNA purification and qPCR.

Patient-like irradiation assays

300,000 T87 and T111 single cells were plated, grown to 100–200 μm spheroids, and either left untreated and incubated for 5 days or treated with 2 Gy of radiation per day, for a total of 5 days. The irradiation was conducted using the CP-160 X-Ray Irradiation System from Faxitron. Both control and treated conditions were partially harvested for RNA purification and qPCR at three different timepoints after the last round of irradiation: 48, 72 and 178 h. mRNA abundance for each timepoint was normalized to the corresponding control harvested at the same timepoint.

Generation of CRISPR-Cas9 KO spheroid cultures

Generation of stable Cas9 expressing glioblastoma spheroid cultures

The T87 and T111 patient-derived models were respectively infected with Lenti-Cas9-2A-Blast and Lenti-PGK-Cas9-P2A-HygR viruses. For each model, 100 000 cells were seeded per well as single cells in a non-treated 24-well plate (Sarstedt #83.3922500) and transduced the same day with lentiviral particles at a MOI of 1 to 10 in the presence of 0.8 μg/mL polybrene (Sigma Aldrich #TR-1003-G). Twenty-four hours post-transduction, medium was changed. Forty-eight hours later, the T87 and T111 Cas9 cells were respectively selected with 10 μg/ml of blasticidin (ChemCruz #SC495389) or 200 μg/ml of hygromycin B (ThermoFisher #83.3922500). Antibiotic resistance-selected cells were expanded 1 week after treatment.

The CRISPR-Cas9 genome editing capability of T87Cas9 and T111 Cas9 cells was tested by transfecting a sgRNA targeting WEE1. WEE1 is an essential gene for survival and thus, cells that have undergone gene

editing at the WEE1 locus die within a few days. T87Cas9 and T111Cas9 cells were seeded in 384-well plates (Corning #4588) and transfected with the WEE1 sgRNA (Horizon #SQ-005050-01-0002) or 2 non-targeting control sgRNAs (Horizon #U-009501-01-02 and U-009503-01-02) using lipofectamine RNAiMax (Thermo Fisher #13,778,075) the same day. Ninety-six hours later, cell viability was determined using CellTiter-Glo 2.0 cell viability assay (Promega #G9242) according to the manufacturer instructions. Cell viability was normalized to non-targeting controls and cells transfected with the WEE1 sgRNA displayed low viability (< 30%) indicating efficient gene editing.

Virus production

The HEK 293-FT cells were seeded at 1×10^5 cells per cm^2 16 h prior to transfection. Transfection of Cas9 plasmids (Addgene #73,310 #164,135) and packaging plasmids MD2.G (Addgene # 12,259) and psPAX2(Addgene #12,260) was done using Lipofectamine 2000 transfection reagent (ThermoFisher #11,668,027) according to the manufacturer's protocol. Viral supernatant was collected 48 h post-transfection and the titer was assessed according to Stewart et al.⁴¹.

GDNF and GFRA1 KO transfection

T87 Cas 9 and T111 Cas9 modified spheroid cultures were grown in NB medium supplemented with hygromycin (200 $\mu\text{g}/\text{ml}$) or blasticidin (10 mg/ml) respectively for 2 weeks at 37 °C in a humidified atmosphere of 5% CO_2 , to select Cas9 expressing cells, before proceeding with the transfection.

One non-targeting control (NTC1), three GDNF KO and three GFRA1 KO Edit-R predesigned synthetic sgRNAs were purchased from Horizon Discovery (NTC1: U-009501-01-02, GDNF: SQ-011040-01-0002, GFRA1: SQ-007913-01-0002). For each transfection, 5 pmol of the sgRNAs dissolved in 10 mM Tris HCl Buffer pH 7.4 (Horizon Discovery) were transfected into the cells using 7.5 μl of Lipofectamine RNAiMAX (ThermoFisher Scientific) resuspended in 150 μl Opti-MEM reduced serum media (ThermoFisher Scientific). 500,000 cells per condition were incubated in the transfection mix for 5 h before harvesting. The transfected cells were resuspended in 5 ml NB media and seeded in T25 flasks. To test the viability of the NTC and KO cells, 25,000 cells of NTC1 and all KO conditions were seeded in 96-well plates and incubated at 37 °C and 5% CO_2 for 5 days. MTT viability testing was done by adding 10 μl of Thiazolyl Blue Tetrazolium Bromide (5 mg/ml , MTT, Sigma-Aldrich) per well and incubating for 4 h, before adding 100 μl of MTT solubilization buffer (10% SDS; 0.01 M HCl).

ELISA

For both T87 and T111, 6 million cells of NTC1 and all three GDNF-KO models, were seeded in 30 mL of media and cultured at 37 °C in a humidified atmosphere of 5% CO_2 for a week, after which the conditioned culture media was concentrated with Pierce Protein Concentrators 10 K MWCO (ThermoFisher Scientific), and the GDNF ELISA assays were conducted using the Human GDNF Quantikine ELISA kit from R&D Systems.

Treatment viability assays of the KO spheroid cultures

For both T87 and T111, 10,000 NTC1, GDNF-KO and GFRA1-KO single cells were seeded in 96-well plates and incubated for 48 h at 37 °C in a humidified atmosphere of 5% CO_2 before treating with 3 Gy of irradiation, 150 μM temozolomide, 20 μM lomustine or a corresponding DMSO control. MTT viability testing was done 5 days after treatment, following the procedure described previously, in the generation of the KO spheroid models. Relative post-treatment viability of the spheroid cultures was calculated relative to the respective non-treated controls.

GDNF rescue experiment

For both T87 and T111, 10,000 NTC1 and GDNF-KO single cells were seeded in 96-well plates and incubated for 48 h at 37 °C in a humidified atmosphere of 5% CO_2 before treating with 150 μM temozolomide, 20 μM lomustine or a corresponding DMSO control. Half of the wells were treated with 1 $\mu\text{g}/\text{ml}$ of Human Recombinant GDNF (Alomone Labs) 2, 4 and 6 days after seeding. The other half of the wells were treated with a similar MilliQ water dilution in NB media, to act as a control. MTT viability testing was done 7 days after seeding, as per the previously described protocol.

Western blot

Sample preparation

Cell lysates were prepared from the T87 and T111 NTC1 and GFRA1-KO spheroid cultures. 1 million cells of each condition were harvested, centrifuged at 1500 rpm for 5 min to remove the culture media, washed with ice-cold PBS, and resuspended with 100 μl of Pierce RIPA Lysis and Extraction buffer (ThermoFisher Scientific) supplemented with 1X of protease inhibitor (ThermoFisher Scientific) and 4X of phosphatase inhibitor (PhosSTOP, Merck). The cell suspensions were kept on ice and vortexed briefly every 5 min for a total of 40 min, before centrifuging at 15,000 rpm and 4 °C for 30 min and retrieving the supernatant containing the protein lysate. Protein concentration was determined using the Pierce BCA Protein Assay Kit from ThermoFisher Scientific.

Immunoblot

Lysate dilutions were prepared to a final concentration of 0.5 μl and run using the Jess digital western blotting system from Biotechne (PS-ST02EZ-8, SM-W002). This system does not run a full gel, each sample is added to individual capillaries that contain concentration and separation gels. All capillaries undergo the Western Blot assay process at the same time in the Jess machine. We used 1:200 dilutions of the following mouse antibodies

as primary antibodies: β -actin (A5441 AC-15, Merck) and GFRA1 (sc-271546 E-11, Santa Cruz Biotechnology). The secondary antibody and remaining reagents were included in the anti-mouse detection module for Jess (DM-002, Biotechne) and the manufacturer's guidelines were followed. Data was analyzed using the Compass for Simple Wester 6.2.0 Software (Biotechne). The readout of the Jess machine is pictures of each of the individual capillaries after revelation, and not a full gel.

Statistical analysis

Group comparisons were performed using one-way ANOVA or two-way ANOVA test. Error bars represent mean \pm SEM. All statistical analyses and graphs were done using Graph Pad Prism 10 (GraphPad software, San Diego, CA). Statistical significance was defined as $*p < 0.5$, $**p < 0.01$, $***p < 0.001$, $****p < 0.0001$.

Data availability

The RNA-Seq data generated and analyzed during the current study is available in the Gene Expression Omnibus repository, with the GEO accession number GSE255581. All the data used are provided in this article and are available upon reasonable written request. Please contact Bjarne W. Kristensen (Bjarne.winther.kristensen.01@regionh.dk).

Received: 26 January 2024; Accepted: 25 July 2024

Published online: 31 July 2024

References

- Schwartzbaum, J. A., Fisher, J. L., Aldape, K. D. & Wrensch, M. Epidemiology and molecular pathology of glioma. *Nat. Clin. Pract. Neurol.* **2**, 494–503. <https://doi.org/10.1038/ncpneuro0289> (2006).
- Stupp, R. *et al.* Radiotherapy plus concomitant and adjuvant temozolomide for glioblastoma. *N. Engl. J. Med.* **352**, 987–996. <https://doi.org/10.1056/NEJMoa043330> (2005).
- Carr, M. T. *et al.* Comorbid medical conditions as predictors of overall survival in glioblastoma patients. *Sci. Rep.* **9**, 20018. <https://doi.org/10.1038/s41598-019-56574-w> (2019).
- Weller, M. & Le Rhun, E. How did lomustine become standard of care in recurrent glioblastoma?. *Cancer Treat. Rev.* **87**, 102029. <https://doi.org/10.1016/j.ctrv.2020.102029> (2020).
- Bette, S. *et al.* Retrospective analysis of radiological recurrence patterns in glioblastoma, their prognostic value and association to postoperative infarct volume. *Sci. Rep.* **8**, 4561. <https://doi.org/10.1038/s41598-018-22697-9> (2018).
- Lee, C. A. A. *et al.* Targeting the ABC transporter ABCB5 sensitizes glioblastoma to temozolomide-induced apoptosis through a cell-cycle checkpoint regulation mechanism. *J. Biol. Chem.* **295**, 7774–7788. <https://doi.org/10.1074/jbc.RA120.013778> (2020).
- Ou, A., Yung, W. K. A. & Majd, N. Molecular mechanisms of treatment resistance in glioblastoma. *Int. J. Mol. Sci.* <https://doi.org/10.3390/ijms22010351> (2020).
- Chen, X. *et al.* A novel enhancer regulates MGMT expression and promotes temozolomide resistance in glioblastoma. *Nat. Commun.* **9**, 2949. <https://doi.org/10.1038/s41467-018-05373-4> (2018).
- Ledda, F., Paratcha, G., Sandoval-Guzmán, T. & Ibáñez, C. F. GDNF and GFRA1 promote formation of neuronal synapses by ligand-induced cell adhesion. *Nat. Neurosci.* **10**, 293–300. <https://doi.org/10.1038/nn1855> (2007).
- Duarte Azevedo, M., Sander, S. & Tenenbaum, L. GDNF, a neuron-derived factor upregulated in glial cells during disease. *J. Clin. Med.* <https://doi.org/10.3390/jcm9020456> (2020).
- Kawai, K. & Takahashi, M. Intracellular RET signaling pathways activated by GDNF. *Cell Tissue Res.* **382**, 113–123. <https://doi.org/10.1007/s00441-020-03262-1> (2020).
- Airaksinen, M. S. & Saarma, M. The GDNF family: Signalling, biological functions and therapeutic value. *Nat. Rev. Neurosci.* **3**, 383–394. <https://doi.org/10.1038/nrn812> (2002).
- Cintrón-Colón, A. F., Almeida-Alves, G., Boynton, A. M. & Spitsbergen, J. M. GDNF synthesis, signaling, and retrograde transport in motor neurons. *Cell Tissue Res.* **382**, 47–56. <https://doi.org/10.1007/s00441-020-03287-6> (2020).
- Treanor, J. J. S. *et al.* Characterization of a multicomponent receptor for GDNF. *Nature* **382**, 80–83. <https://doi.org/10.1038/382080a0> (1996).
- Paratcha, G., Ledda, F. & Ibáñez, C. F. The neural cell adhesion molecule NCAM is an alternative signaling receptor for GDNF family ligands. *Cell* **113**, 867–879. [https://doi.org/10.1016/S0092-8674\(03\)00435-5](https://doi.org/10.1016/S0092-8674(03)00435-5) (2003).
- Bespalov, M. M. *et al.* Heparan sulfate proteoglycan syndecan-3 is a novel receptor for GDNF, neurturin, and artemin. *J. Cell Biol.* **192**, 153–169. <https://doi.org/10.1083/jcb.201009136> (2011).
- Chen, J. *et al.* Hypothalamic proteoglycan syndecan-3 is a novel cocaine addiction resilience factor. *Nat. Commun.* **4**, 1955. <https://doi.org/10.1038/ncomms2955> (2013).
- Felder, G. C. *et al.* The GDNF family: A role in cancer?. *Neoplasia*. **20**(1), 99–117. <https://doi.org/10.1016/j.neo.2017.10.010> (2018).
- Wiesenhofer, B., Weis, C. & Humpel, C. Glial cell line-derived neurotrophic factor (GDNF) is a proliferation factor for Rat C6 glioma cells: Evidence from antisense experiments. *Antisense Nucl. Acid Drug. Dev.* **10**, 311–321. <https://doi.org/10.1089/oli.1.2000.10.311> (2000).
- Huang, Y. *et al.* Glial cell line-derived neurotrophic factor increases matrix metalloproteinase 9 and 14 expression in microglia and promotes microglia-mediated glioma progression. *J. Neurosci. Res.* **99**, 1048–1063. <https://doi.org/10.1002/jnr.24768> (2021).
- Chen, M., Ba, H., Lu, C., Dai, J. & Sun, J. Glial cell line-derived neurotrophic factor (GDNF) promotes angiogenesis through the demethylation of the fibromodulin (FMOD) promoter in glioblastoma. *Med. Sci. Monit.* **24**, 6137–6143 (2018).
- Ng, W. H., Wan, G. Q., Peng, Z. N. & Too, H. P. Glial cell-line derived neurotrophic factor (GDNF) family of ligands confer chemoresistance in a ligand-specific fashion in malignant gliomas. *J. Clin. Neurosci.* **16**, 427–436. <https://doi.org/10.1016/j.jocn.2008.06.002> (2009).
- Liu, B. *et al.* BMP4 reverses multidrug resistance through modulation of BCL-2 and GDNF in glioblastoma. *Brain Res.* **1507**, 115–124. <https://doi.org/10.1016/j.brainres.2013.02.039> (2013).
- Ku, M.-C. *et al.* GDNF mediates glioblastoma-induced microglia attraction but not astrogliosis. *Acta Neuropathol.* **125**, 609–620. <https://doi.org/10.1007/s00401-013-1079-8> (2013).
- Chen, Q. BMP4 inhibits glioblastoma invasion by promoting E-cadherin and claudin expression. *Front. Biosci.* **24**, 4768. <https://doi.org/10.2741/4768> (2019).
- Song, H. & Moon, A. Glial cell-derived neurotrophic factor (GDNF) promotes low-grade Hs683 glioma cell migration through JNK, ERK-1/2 and p38 MAPK signaling pathways. *Neurosci. Res.* **56**, 29–38. <https://doi.org/10.1016/j.neures.2006.04.019> (2006).

27. Lee, J. *et al.* Tumor stem cells derived from glioblastomas cultured in bFGF and EGF more closely mirror the phenotype and genotype of primary tumors than do serum-cultured cell lines. *Cancer Cell* **9**, 391–403. <https://doi.org/10.1016/j.ccr.2006.03.030> (2006).
28. Rosso, F., Giordano, A., Barbarisi, M. & Barbarisi, A. From cell-ECM interactions to tissue engineering. *J. Cell. Physiol.* **199**, 174–180. <https://doi.org/10.1002/jcp.10471> (2004).
29. Al-Sammarraie, N. & Ray, S. K. Applications of CRISPR-Cas9 technology to genome editing in glioblastoma multiforme. *Cells* **10**, 2342. <https://doi.org/10.3390/cells10092342> (2021).
30. MacLeod, G. *et al.* Genome-Wide CRISPR-Cas9 screens expose genetic vulnerabilities and mechanisms of temozolomide sensitivity in glioblastoma stem cells. *Cell Rep.* **27**, 971–986.e9. <https://doi.org/10.1016/j.celrep.2019.03.047> (2019).
31. Park, J. *et al.* Transcriptome profiling-based identification of prognostic subtypes and multi-omics signatures of glioblastoma. *Sci. Rep.* **9**, 10555. <https://doi.org/10.1038/s41598-019-47066-y> (2019).
32. Ibáñez, C. F. & Andressoo, J.-O. Biology of GDNF and its receptors—Relevance for disorders of the central nervous system. *Neurobiol. Dis.* **97**, 80–89. <https://doi.org/10.1016/j.nbd.2016.01.021> (2017).
33. Wang, Y. *et al.* GDNF triggers proliferation of rat C6 glioma cells via the NF- κ B/CXCL1 signaling pathway. *PLoS One* **18**, e0289071. <https://doi.org/10.1371/journal.pone.0289071> (2023).
34. Fan, T. *et al.* Reciprocal feedback regulation of ST3GAL1 and GFRA1 signaling in breast cancer cells. *Cancer Lett.* **434**, 184–195. <https://doi.org/10.1016/j.canlet.2018.07.026> (2018).
35. Giuliano, C. J., Lin, A., Girish, V. & Sheltzer, J. M. Generating Single cell-derived knockout clones in mammalian cells with CRISPR/Cas9. *Curr. Protoc. Mol. Biol.* <https://doi.org/10.1002/cpmb.100> (2019).
36. Penninckx, S., Pariset, E., Cekanaviciute, E. & Costes, S. V. Quantification of radiation-induced DNA double strand break repair foci to evaluate and predict biological responses to ionizing radiation. *NAR Cancer* <https://doi.org/10.1093/narcan/zcab046> (2021).
37. Luz, M., Mohr, E. & Fibiger, H. C. GDNF-induced cerebellar toxicity: A brief review. *Neurotoxicology* **52**, 46–56. <https://doi.org/10.1016/j.neuro.2015.10.011> (2016).
38. Tong, S.-Y. *et al.* Serum glial cell line-derived neurotrophic factor (GDNF) a potential biomarker of executive function in Parkinson's disease. *Front. Neurosci.* <https://doi.org/10.3389/fnins.2023.1136499> (2023).
39. Straten, G., Eschweiler, G. W., Maetzler, W., Laske, C. & Leyhe, T. Glial cell-line derived neurotrophic factor (GDNF) concentrations in cerebrospinal fluid and serum of patients with early Alzheimer's disease and normal controls. *J. Alzheimer's Dis.* **18**, 331–337. <https://doi.org/10.3233/JAD-2009-1146> (2009).
40. Jensen, S. S., Aaberg-Jessen, C., Andersen, C., Schröder, H. D. & Kristensen, B. W. Glioma spheroids obtained via ultrasonic aspiration are viable and express stem cell markers. *Neurosurgery* **73**, 868–886. <https://doi.org/10.1227/NEU.000000000000118> (2013).
41. Stewart, S. A. *et al.* Lentivirus-delivered stable gene silencing by RNAi in primary cells. *RNA* **9**, 493–501. <https://doi.org/10.1261/rna.2192803> (2003).

Acknowledgements

The authors would like to thank Jan Benada and the Sørensen group at the Biotech Research and Innovation Center (BRIC) for sharing their equipment and expertise in the irradiation experiments. This study was financially supported by the Danish Cancer Society (R281-16494), the Danish Cancer Research Foundation, Neye Fonden, Sofus Carl Emil Friis and wife Olga Doris Fond, Krista og Viggo Petersens Fond, Grosserer Valdemar Foersom, Dagmar Marshall Fond, Fabrikant Einar Willumsens Mindelegat, Brogaard og Hustrus Mindefond, and Tømrermester Jørgen Holm og Hustru Elisa F Hansens Mindelegat.

Author contributions

Conceptualization by B.W.K, S.R.M and J.D.E. Cas9 cell models provided by J.A.B. and K.W. Experiments conducted by I.C.N.A., J.D.E., I.H.K., S.A.P, and M.N.T. Data analysis by M.B. and M.T. Writing of the original draft by I.C.N.A. All authors reviewed the manuscript.

Competing interests

The authors declare no competing interests.

Additional information

Supplementary Information The online version contains supplementary material available at <https://doi.org/10.1038/s41598-024-68626-x>.

Correspondence and requests for materials should be addressed to B.W.K.

Reprints and permissions information is available at www.nature.com/reprints.

Publisher's note Springer Nature remains neutral with regard to jurisdictional claims in published maps and institutional affiliations.



Open Access This article is licensed under a Creative Commons Attribution-NonCommercial-NoDerivatives 4.0 International License, which permits any non-commercial use, sharing, distribution and reproduction in any medium or format, as long as you give appropriate credit to the original author(s) and the source, provide a link to the Creative Commons licence, and indicate if you modified the licensed material. You do not have permission under this licence to share adapted material derived from this article or parts of it. The images or other third party material in this article are included in the article's Creative Commons licence, unless indicated otherwise in a credit line to the material. If material is not included in the article's Creative Commons licence and your intended use is not permitted by statutory regulation or exceeds the permitted use, you will need to obtain permission directly from the copyright holder. To view a copy of this licence, visit <http://creativecommons.org/licenses/by-nc-nd/4.0/>.

© The Author(s) 2024